Exact hidden-surface removal in digitally synthetic full-parallax holograms

doi: 10.1117/12.592520

Exact hidden-surface removal in digitally synthetic full-parallax holograms

K. Matsushima[a]

[a]Department of Electrical Engineering and Computer Science, Kansai University
Yamate-cho 3-3-35, Suita, Osaka 564-8680, Japan

ABSTRACT

A new algorithm for removing hidden surfaces from reconstruction of computer-generated holograms is presented. The object used in the algorithm is defined by surface model and each polygon composing the object provides a mask for blocking the incident field into the backside of the polygon. The computational cost of the proposed algorithm is 2 FFT/polygon by handling field transmission in Fourier space and integrating the surface diffraction method for generating fields. Reconstruction of a hologram synthesized by using the presented algorithm is demonstrated.

Keywords: Hidden surface removal, Computer generated hologram, digitally synthetic hologram, surface diffraction method

1. INTRODUCTION

In the CGHs, algorithms for hidden-surface removal found in literature are either the geometrical method[1,2] suitable for the ray tracing in the point-source model or the wave optical method based on layered model.[3] The former is usually much time-consuming algorithm and only handle horizontal-parallax-only holograms, i.e., it can not deal with full-parallax holograms. The latter, proposed by A. Lohmann, is capable of removing hidden part from reconstruction of full-parallax holograms, but the objects must be sliced in planes parallel to the hologram. Thus, it is difficult to apply some standard rendering techniques used for realistic reconstruction of 3-D objects, such as shading and texture mapping.

In the last meeting, we presented a novel algorithm for hidden-surface removal.[4] The algorithm based on the rotational transformation[5] of wave fields has resulted in a method by silhouette approximation. The presented algorithm is simple in principle and able to using for full-parallax holograms. However, the silhouette approximation is valid under paraxial conditions, i.e., utilization of the silhouette approximation is limited in holograms with narrow viewing zone.

In this report, more exact algorithm is presented for hidden-surface removal. This new method is also based on the rotational transformation of wave fields, as well as the former algorithm, but do not use the Silhouette approximation. The proposed new algorithm rigorously calculates obstruction of the field by a tilted surface.

Further author information:
E-mail: matsu@kansai-u.ac.jp, Telephone/Fax: +81-6-6368-0933

Figure 1. The principle of painter's algorithm.

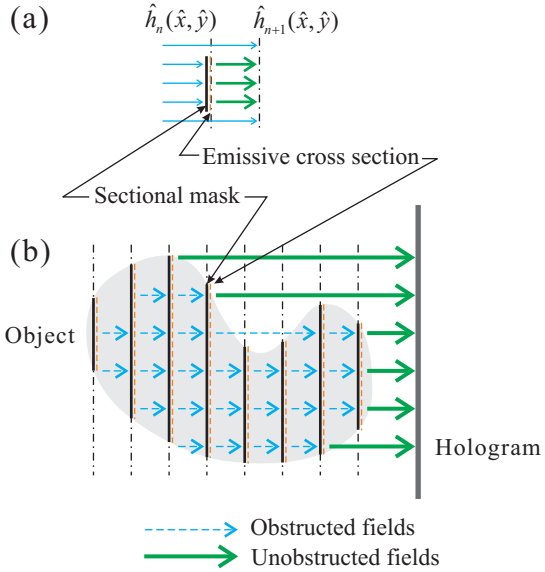

Figure 2. The principle of algorithm used in layered holograms.

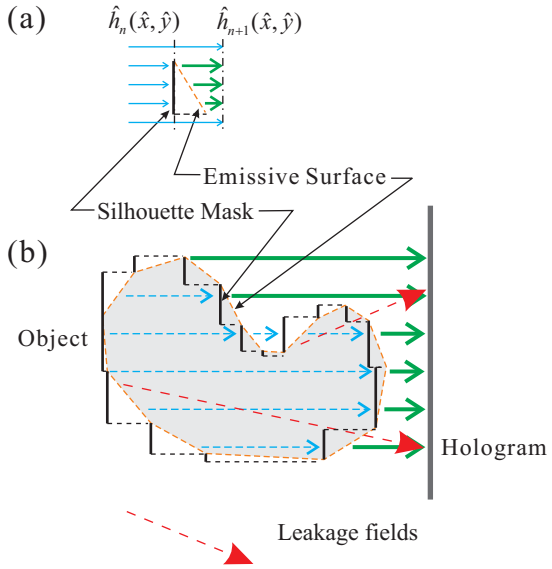

Figure 3. The principle of algorithm based on silhouette approximation.

This kind of rigorous obstruction, in general, leads to a high computational cost. For example, it requires FFT operation four times to process field-obstruction by a surface. However, the presented algorithm can reduce the computational cost to 2 FFT/Surface by handling field transmission in Fourier space instead of real space.

2. LAYERED HOLOGRAMS AND SILHOUETTE APPROXIMATION

Painter's algorithm, a well-known method for removing hidden surface in the field of computer graphics (CG), gets its name from the process that painters render a scene in paints. Fig.1 (a)–(c) show the principle of painter's algorithm. An artist might draws the background scenery such as mountains or a forest in their canvas first and the foreground objects last. This is a very simple and primitive method for hidden surface removal.

Mechanism of hidden surface removal in layered holograms and algorithm by using the silhouette approximation[4] are analogous with the painter's algorithm. In these methods, an object is composed of planes, i.e. planar surfaces or cross sections. These planes are sorted by depth so that the calculation of the object fields proceeds from farthest to closest to the hologram.

2.1. Layered holograms

An object sliced in several planes parallel to the hologram. The planes are sorted in depth order, and each cross section functions as a mask blocking the incident field and plays the role of a light source. The planes are numbered 1 to N from farthest to closest to the hologram. When a field $\hat{h}_n(\hat{x},\hat{y})$ comes into the nth plane as shown in Fig.2 (a), field passing through the nth plane is given by

$$\hat{h}'(\hat{x},\hat{y}) = \hat{h}_n(\hat{x},\hat{y})\hat{m}_n(\hat{x},\hat{y}), \tag{1}$$

where $\hat{m}_n(\hat{x},\hat{y})$ is a mask function that is unity within the cross section of the object or zero otherwise.

A cross section works not only as the mask but also a light source. If complex amplitudes of the light source on a cross section is given by $\hat{o}(\hat{x},\hat{y})$ in the nth plane. The incident field of the $(n+1)$th plane is written as

$$\begin{aligned}\hat{h}_{n+1}(\hat{x},\hat{y}) &= \mathrm{P}_{d_n}\{\hat{h}'_n(\hat{x},\hat{y}) + \hat{o}_n(\hat{x},\hat{y})\} \\ &= \mathrm{P}_{d_n}\{\hat{h}_n(\hat{x},\hat{y})\hat{m}_n(\hat{x},\hat{y}) + \hat{o}_n(\hat{x},\hat{y})\},\end{aligned} \tag{2}$$

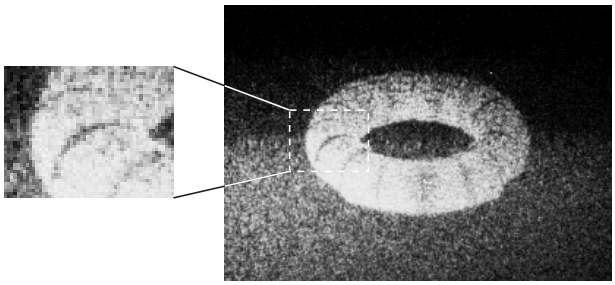

Figure 4. Gaps owing to leakage fields between silhouette masks.[4]

where $\mathrm{P}_d\{u(\hat{x},\hat{y})\}$ is defined as the propagation operator of the field $u(\hat{x},\hat{y})$ in distance d.

The object field is calculated from $\hat{h}_1(\hat{x},\hat{y}) = \hat{o}_1(\hat{x},\hat{y})$ to $\hat{h}_N(\hat{x},\hat{y})$ as if an artist paints his picture, as shown in Fig.2 (b), and finally obtained in the hologram plane as follows:

$$\hat{h}_{\mathrm{Hologram}}(\hat{x},\hat{y}) = \mathrm{P}_{d_N}\{\hat{h}_N(\hat{x},\hat{y})\hat{m}_N(\hat{x},\hat{y}) + \hat{o}_N(\hat{x},\hat{y})\}. \tag{3}$$

2.2. Silhouette approximation in surface objects

Main drawback of the simple layered holograms is that object must be sliced in a set of planes parallel to the hologram. Since any surfaces are not defined in this object model, it is difficult to render the object by using several major techniques such as shading or texture mapping.

For surface objects, ray-oriented algorithm for hidden surface removal has been reported in several literature, but these are generally too slow to apply for full-parallax holograms, and therefore, used only for horizontal parallax only holograms.

Algorithm based on silhouette approximation was proposed for full-parallax synthetic holograms of surface objects. The idea is very simple. Suppose that an object is constructed of many planar surface, polygon, and numbered in order of depth. A part of the incident field into backside of a polygon is clipped out by a mask that is the silhouette of the polygon as shown in Fig. 3 (a).

The field obstructed by the silhouette mask is given as

$$\hat{h}'_n(\hat{x},\hat{y}) = \hat{h}_n(\hat{x},\hat{y})\hat{m}_{s,n}(\hat{x},\hat{y}), \tag{4}$$

where $\hat{m}_{s,n}(\hat{x},\hat{y})$ denotes a function of the silhouette mask for the nth surface, which is the silhouette of the polygon onto a plane parallel to the hologram.

The field emitted from the polygon itself must be calculated by using some ordinal methods, for example, superposition of spherical waves from point sources filled in the polygon. Suppose that the field generated from the nth polygon is given as $O(\hat{x},\hat{y})$ in the next $(n+1)$th plane. The recurrence formula is given as follows:

$$\hat{h}_{n+1}(\hat{x},\hat{y}) = \mathrm{P}_{d_n}\{\hat{h}_n(\hat{x},\hat{y})\hat{m}_{s,n}(\hat{x},\hat{y})\} + O(\hat{x},\hat{y}). \tag{5}$$

2.3. Rigorous hidden surface removal for surface objects

If the field is paraxial, i.e. the light propagate almost along the optical axis, the silhouette approximation is a good trade-off between the computational cost and quality of the reconstructed image. However, if viewing zone of a hologram is enough large for the hologram to reconstruct the auto-stereoscopic image, the field is no longer paraxial, and therefore leakage fields passing through the gap between silhouette masks increase as shown in Fig. 3 (b).

An example of leakage of fields is shown in Fig. 4. In this case, the light emitted from the farside of the object passes through the inside of the object and is observed in reconstruction. Since the light from the farside

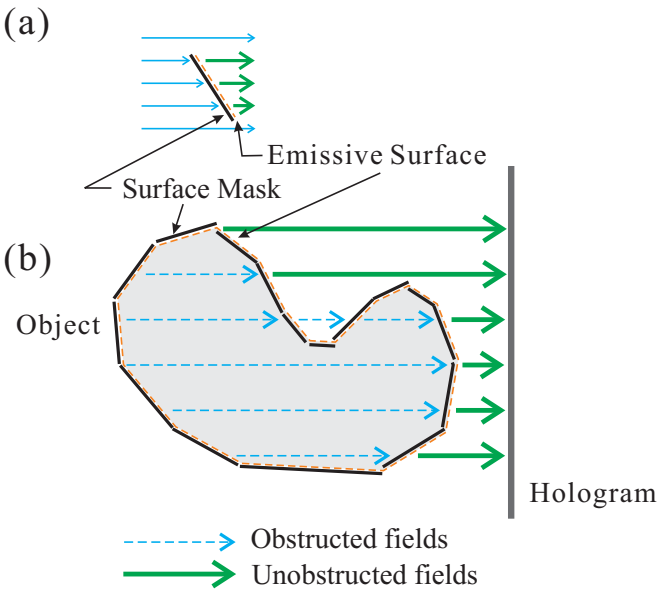

Figure 5. The principle of complete blocking the fields that should be obstructed.

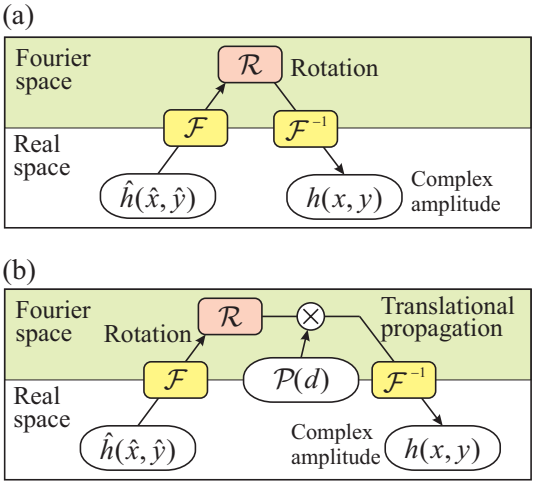

Figure 6. A diagram of steps to perform rotational transformation without (a) and with (b) translational propagation.

spreads inside the object and its intensity is weaker than that on the surface of the nearside, the leakage field is observed as a dark gap between polygons.

More exact methods are required for preventing leakage and blocking the fields completely. Fig. 5 shows the principle of the exacter method. An incident field into the backside of a polygon is obstructed by a tilted mask, of which shape and position is same as the polygon itself. There is not any gap that fields pass through.

An procedure for realizing the fields obstruction by tilted masks is described in the following section.

3. OBSTRUCTION BY A TILTED PLANE

We have already reported the basic procedure for obstruction by a tilted mask in the last meeting (Ref. 4). Let us summarize this for convenience bellow.

3.1. Rotational transformation

Complex amplitudes of an incident field in a plane not parallel to the hologram must be obtained to block the incident field by a tilted polygon. The rotational transformation of a field given in a local parallel plane $(\hat{x}, \hat{y}, \hat{z} = 0)$ is written as

$$h(x, y) = \mathcal{F}^{-1}\mathcal{R}_{\psi}\mathcal{F}\{\hat{h}(\hat{x}, \hat{y})\}, \tag{6}$$

where $(x, y, z = 0)$ is a tilted plane in which a polygon is laid and $h(x, y)$ is the complex amplitudes of the field on it. Here, $\mathcal{F}\{\cdot\}$ and $\mathcal{F}^{-1}\{\cdot\}$ denote Fourier and inverse Fourier transformation, respectively, as follows:

$$\hat{H}(\hat{u}, \hat{v}) = \mathcal{F}\{\hat{h}(\hat{x}, \hat{y})\}, \tag{7}$$

$$h(x, y) = \mathcal{F}^{-1}\{H(u, v)\}. \tag{8}$$

where $(\hat{u}, \hat{v})$ and (u, v) are Fourier coordinates in the parallel and the tilted plane to the hologram, respectively. Suppose that a transformation matrix for coordinates rotation is defined as

$$\begin{pmatrix} \hat{x} \\ \hat{y} \\ \hat{z} \end{pmatrix} = \mathbf{T}_{\psi} \begin{pmatrix} x \\ y \\ z \end{pmatrix}, \quad \mathbf{T}_{\psi} = \begin{pmatrix} \hat{a}_1 & \hat{a}_2 & \hat{a}_3 \\ \hat{a}_4 & \hat{a}_5 & \hat{a}_6 \\ \hat{a}_7 & \hat{a}_8 & \hat{a}_9 \end{pmatrix}. \tag{9}$$

Rotational transformation in Fourier space is given as

$$H(u,v) = \mathcal{R}_\psi\{\hat{H}(\hat{u},\hat{v})\} \tag{10}$$

$$= \hat{H}(\hat{a}_1 u + \hat{a}_2 v + \hat{a}_3 w(u,v), \hat{a}_4 u + \hat{a}_5 v + \hat{a}_6 w(u,v)), \tag{11}$$

where $w(u,v)$ is Fourier frequency in z direction perpendicular to the tilted plane and given by

$$w(u,v) = \sqrt{\lambda^{-2} - u^2 - v^2}. \tag{12}$$

The computational process for the rotational transformation is summarized as a diagram shown in Fig. 6 (a).

If translational propagation of the field follows rotational transformation, the propagated field after rotation is given by

$$h(x,y) = \mathcal{F}^{-1}\left\{\mathcal{R}_\psi \mathcal{F}\{\hat{h}(\hat{x},\hat{y})\} \times \mathcal{P}(d)\right\}, \tag{13}$$

where $\mathcal{P}(d) = \exp[i2\pi d(\lambda^{-2} - u^2 - v^2)^{1/2}]$ is the phase factor in Fourier space to propagate the field translationally for a distance of d.[6] The diagram for the rotational transformation followed by translational propagation is shown in Fig. 6 (b).

3.2. Masking fields in the tilted plane

Fig. 7 (a) shows the procedure for masking a field in a tilted plane. The mask function for the polygon must be multiplied by the incident field in the tilted plane that the polygon laid on. Therefore, when the field $\hat{h}_n(\hat{x},\hat{y})$ denotes the incident field into the backside of the nth polygon, the obstructed field is given by use of eq. (6) as follow:

$$h'_n(x,y) = \mathcal{F}^{-1}\mathcal{R}_{-\psi_n}\mathcal{F}\{\hat{h}_n(\hat{x},\hat{y})\} \times m_n(x,y). \tag{14}$$

Complex amplitudes of the obstructed field in a plane parallel to the hologram is obtained by inverse rotation of $h'(x,y)$.

$$\hat{h}'_n(\hat{x},\hat{y}) = \mathcal{F}^{-1}\mathcal{R}_{+\psi_n}\mathcal{F}\{h'_n(x,y)\}$$

$$= \mathcal{F}^{-1}\mathcal{R}_{+\psi_n}\mathcal{F}\left\{\mathcal{F}^{-1}\mathcal{R}_{-\psi_n}\mathcal{F}\{\hat{h}_n(\hat{x},\hat{y})\} \times m_n(x,y)\right\} \tag{15}$$

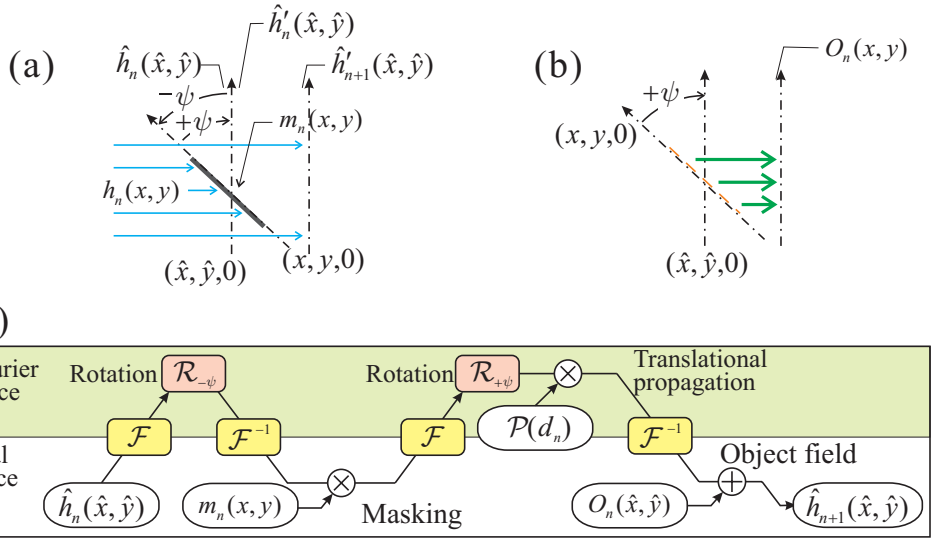

Figure 7. The procedure for exact hidden surface removal: masking (a) and generating (b) a field, and the diagram for computation(c).

Furthermore, the obstructed field in the next plane is given by substituting $h'_n(x,y)$ of eq. (14) into (13) instead of $\hat{h}(\hat{x},\hat{y})$ as follows:

$$\hat{h}'_{n+1}(\hat{x},\hat{y}) = \mathcal{F}^{-1}\left\{\mathcal{R}_{+\psi_n}\mathcal{F}\left\{\mathcal{F}^{-1}\mathcal{R}_{-\psi_n}\mathcal{F}\{\hat{h}_n(\hat{x},\hat{y})\}\times m_n(x,y)\right\}\times\mathcal{P}(d)\right\} \tag{16}$$

As a result, the recurrence formula is given by

$$\begin{aligned}\hat{h}_{n+1}(\hat{x},\hat{y}) &= \hat{h}'_{n+1}(\hat{x},\hat{y}) + O_n(\hat{x},\hat{y})\\ &= \mathcal{F}^{-1}\left\{\mathcal{R}_{+\psi_n}\mathcal{F}\left\{\mathcal{F}^{-1}\mathcal{R}_{-\psi_n}\mathcal{F}\{\hat{h}_n(\hat{x},\hat{y})\}\times m_n(x,y)\right\}\times\mathcal{P}(d_n)\right\} + O_n(\hat{x},\hat{y}),\end{aligned} \tag{17}$$

where $O_n(\hat{x},\hat{y})$ given in the $(n+1)$ plane is again the field emitted from the nth polygon as shown in Fig. 7 (b). Computational procedure for calculating eq. (17) is indicated as a diagram shown in Fig. 7 (c)

4. COMBINATION WITH THE SURFACE DIFFRACTION METHOD

A wave optical method to generate fields emitted from a surface object has been proposed.[7,8] In the method, called surface diffraction method, an object are composed of some polygons, and fields from each polygons are calculated by using the rotational transformation mentioned above. Therefore, the surface diffraction method has close affinity with the method for hidden surface removal described in the previous section.

In the surface diffraction method, each polygon has its own complex function $s_n(x,y)$, called the property function of the surface, to keep characteristics of the polygon such as the shape and texture. The field emitted from a polygon is calculated by rotational transformation and propagation of eq. (13).

$$O_n(\hat{x},\hat{y}) = \mathcal{F}^{-1}\left\{\mathcal{R}_{-\psi_n}\mathcal{F}\left\{s_n(x,y)\right\}\times\mathcal{P}(d_n)\right\}. \tag{18}$$

Recurrence formula can be rewritten by substituting eq. (18) into (17) as follows:

$$\hat{h}_{n+1}(\hat{x},\hat{y}) = \mathcal{F}^{-1}\left\{\mathcal{R}_{+\psi_n}\mathcal{F}\left\{\mathcal{F}^{-1}\mathcal{R}_{-\psi_n}\mathcal{F}\{\hat{h}_n(\hat{x},\hat{y})\}\times m_n(x,y)+s_n(x_n,y_n)\right\}\times\mathcal{P}(d_n)\right\}. \tag{19}$$

Fourier transform appears four times in eq. (19). However, the number of times performing Fourier transform can be reduced by Fourier transform of both sides and substituting eq. (7) into (19). The recurrence formula of complex amplitudes is rewritten as that of spectrum of the field as follows:

$$\hat{H}_{n+1}(\hat{u},\hat{v}) = \mathcal{R}_{+\psi_n}\mathcal{F}\{\mathcal{F}^{-1}\mathcal{R}^{-1}_{-\psi_n}\{\hat{H}_n(\hat{u},\hat{v})\}m_n(x_n,y_n)+s_n(x_n,y_n)\}\times\mathcal{P}(d_n). \tag{20}$$

The total field on the hologram is given by

$$h_{\mathrm{Hologram}}(\hat{x},\hat{y}) = \mathcal{F}^{-1}\{\hat{H}_{N+1}(\hat{u},\hat{v})\}. \tag{21}$$

The diagram for numerical calculation of eq. (20) is shown in Fig. 8. In this case, wave fields is handled in its spectrum $\hat{H}(\hat{u},\hat{v})$, i.e. the field is transmitted from a segment to the next in Fourier space. As a result, the recurrence formula is simplified and the number of times performing FFT is reduced in compared with field transmission in real space. The computational cost is estimated as 2 FFT/polygon in this algorithm.

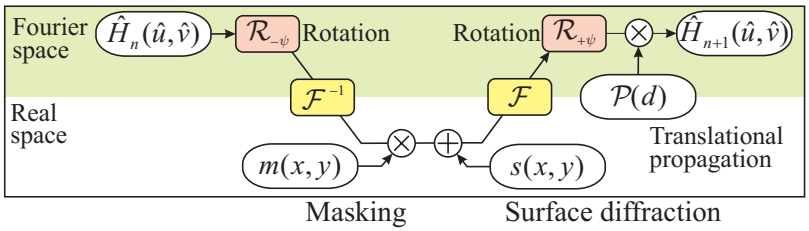

Figure 8. The diagram for the procedure of computation by using field transmission in Fourier space.

5. SORTING POLYGONS

Polygons must be numbered in order of the depth before starting calculation by the recurrence formula of eq. (20). However, determining the order is not always easy depending on disposition of polygons. Fig. 9 shows how determine which polygon to be processed first. In Fig. 9 (a), polygons do not obscure each other, because one polygon is placed outside the maximum region of the field emitted from the other. The maximum region can be obtained from the maximum angle of diffraction θ_d. The polygon P_2 partially obscure P_1 in (b), while P_2 completely obstructs the field from P_1 in (c).

Fig. 9 (c) shows some cases in which it is complicated to determine the order of processing. However, even in these cases, we usually be able to judge the order by use of information on the position of the intersection of one polygon and the extension of the other (P_1 and P_2), or the intersection of one polygon and the normal vector of the other(P_3 and P_4).

Several cases, in which the judgment of the processing order fails, are shown in Fig. 10. The case shown in (a) is commonly known in the painter's algorithm of CG. The processing order of polygons can not be defined because polygons cyclically obscure each other. The case in (b) is peculiar to this algorithm; each of the polygons obstructs the other's field. In the both cases, it is necessary to divide a polygon into several pieces.

6. FABRICATION AND RECONSTRUCTION OF A HOLOGRAM

A hologram, of which the object field were synthesized by using eq. (20), was fabricated and optically reconstructed. Number and sizes of pixels of the hologram are 16384 × 4096 and 1.5μm×2.0μm, respectively. Wavelength for reconstruction is 633nm.

Fig. 11 shows the object model. There are three planes: one is a black and white check pattern as the background, and the others are gray triangles that are rotated at angles of 60 or 80 degree for the hologram.

Fig. 12 shows optical reconstruction of the hologram. The observed images change in (a) and (b) as the viewpoint moves left and right. Therefore, the effect of the proposed algorithm for hidden surface removal can be verified.

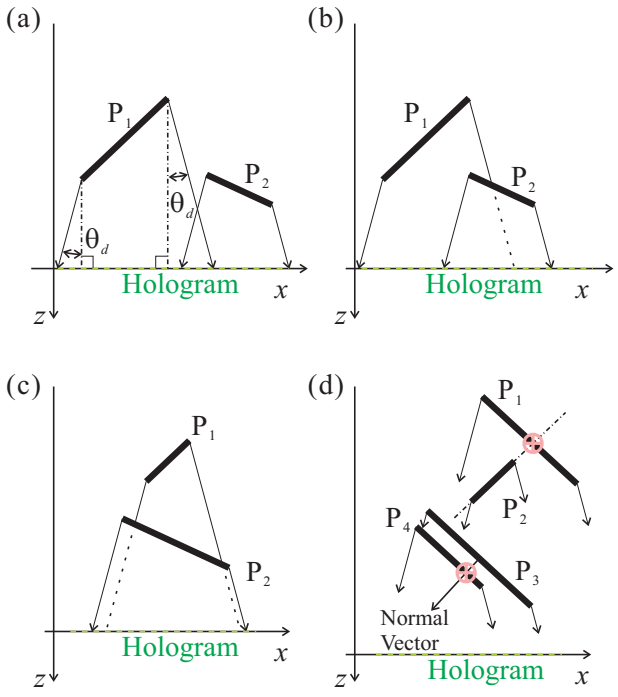

Figure 9. Some cases that one polygon obscures the other (a)–(c) and judgment of the order is complicated (d).

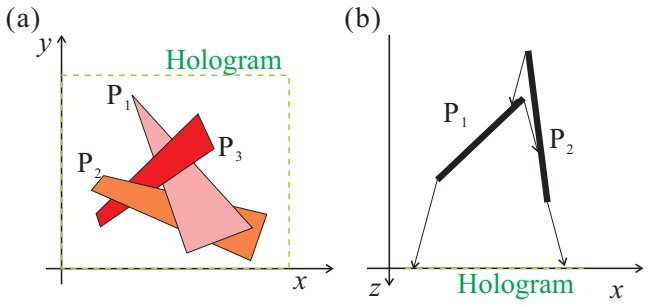

Figure 10. Two cases in which the sequence of processing polygons fails to be determine.

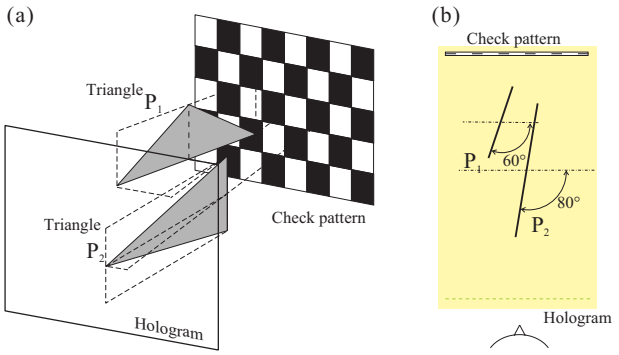

Figure 11. The object model in bird's view (a) and top view (b).

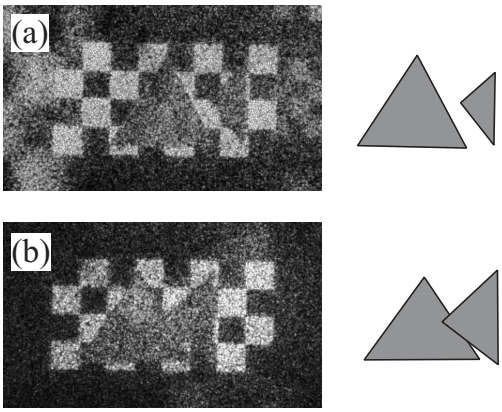

Figure 12. Optical reconstruction of the fabricated hologram.

7. CONCLUSION

In conclusion, algorithm for hidden surface removal, which is more exact than the silhouette approximation, has been proposed. Unlike the silhouette approximation, in the presented algorithm, the incident field into the backside of a tilted polygon is blocked by the tilted mask with the same shape of the polygon. As a result, any leakage field does not occur even in synthetic holograms with a extremely large viewing zone.

Rotational transformation must be performed twice to process field obstruction of a tilted polygon. This leads to execute FFT four times to process a surface. However, handling the field transmission in Fourier space instead of real space makes it possible to decrease the number of times executing FFT.

Furthermore, the presented algorithm has a high compatibility with the surface diffraction method to generate fields from tilted surfaces. As a result, the computational cost for hidden surface removal by the presented algorithm is reduced to 2 FFT/polygon by integrating the surface diffraction method.

REFERENCES

1. J. Underkoffler, "Occlusion processing and smooth surface shading for fully computed synthetic holography," *SPIE Proc. Practical Holography XI* **3011**, pp. 19–29, 1997.
2. T. Hamano and M. Kitamura, "Computer-generated holograms for reconstructing multi-3-D images by space-division recording method," *SPIE Proc. Practical Holography XIV and Holographic Materials VI* **#3956**, pp. 23–32, 2000.
3. A. W. Lohmann, "Three-dimensional properties of wave-fields," *Optik* **51**, pp. 105–117, 1978.
4. K. Matsushima and A. Kondoh, "A wave optical algorithm for hidden-surface removal in digitally synthetic full-parallax holograms for three-dimensional objects," *SPIE Proc. Practical Holography XVIII* **#5290**, p. 90, 2004.
5. K. Matsushima, H. Schimmel, and F. Wyrowski, "Fast calculation method for optical diffraction on tilted planes by use of the angular spectrum of plane waves," *J. Opt. Soc. Am.* **A20**, pp. 1755–1762, 2003.
6. J. W. Goodman, *Introduction to Fourier Optics, 2nd ed.*, ch. 3.10. McGraw-Hill, 1996.
7. K. Matsushima and A. Kondoh, "Wave optical algorithm for creating digitally synthetic holograms of three-dimensional surface objects," *SPIE Proc. Practical Holography XVII and Holographic Materials IX* **#5005**, pp. 190–197, 2003.
8. K. Matsushima, "Computer-generated holograms for three-dimensional surface objects with shade and texture," *Appl. Opt.* , 2005. in press.